CIRCULAR CONCRETE COLUMNS REINFORCED WITH STEEL AND GFRP UNDER SIMULATED EARTHQUAKE LOADS

Arsalan Tavassoli
M.A.Sc. Candidate, University of Toronto, Canada
Arsalan.tavassoli@mail.utoronto.ca

Shamim A. Sheikh
Professor, University of Toronto, Canada
sheikh@ecf.utoronto.ca

Abstract: To address the issue of corrosion of steel in concrete structures, GFRP is slowly gaining acceptability as a replacement of steel. In an effort to evaluate the feasibility of GFRP bars and spirals as internal reinforcement in columns, an extensive research program is underway at the University of Toronto. A total of seventeen 356 mm diameter concrete columns have been tested under simulated earthquake forces which included constant axial load and cyclic lateral displacement excursions. All columns were reinforced laterally with GFRP spirals. Nine columns contained longitudinal GFRP bars while eight had longitudinal steel bars. Results from a select group of specimens are presented in this paper in the form of moment vs. curvature response and shear vs. lateral deflection behaviour. A number of ductility parameters related to curvature, displacement, and energy dissipation are used to evaluate the performance of specimens. Columns containing longitudinal and lateral GFRP reinforcement demonstrated a stable post elastic response accompanying large deformability. Columns reinforced with longitudinal steel and GFRP spirals also displayed excellent behaviour with higher stiffness and larger shear and moment capacities. Large deformability was obtained mainly due to the linear elastic behaviour of GFRP spirals until rupture at a strain of approximate 0.02.

1 Introduction

The annual cost of corrosion from all sectors worldwide in 2010 was estimated at USD 2.2 trillion which is about 3% of the world's GDP of USD 73.33 trillion (NACE-International, 2010). A typical case of corrosion happens in bridge decks, beams and columns. In general, corrosion is the result of water with a low pH. A layer of calcium carbonate is formed on the surface of concrete through the reaction between carbon dioxide and the moisture. The formed layer slowly spreads deeper into concrete. Calcium carbonate decreases the alkalinity of concrete which allows corrosion of the steel bar. As the steel continues to corrode, the buildup of rusts puts pressure on the surrounding concrete, causing cracking around the steel. Eventually, the expansion due to corrosion causes the concrete to spall off.

An important feature of fiber reinforced polymer composites (FRP) is their high corrosion resistance property. This characteristic of non-metallic bars makes them suitable for use in structures subjected to corrosive environmental exposures. For instance, use of FRP bars as internal reinforcement in concrete structural members in parking garages, multistory buildings, industrial structures, and bridges can improve their durability significantly.

Glass fiber reinforced polymer (GFRP) bars in member subjected to mostly flexure have been an active research area over the last several years. But a limited number of tests on GFRP reinforced concrete columns have been reported and they showed that the column specimens behaved reasonably strong with a large amount of ductility. Columns with GFRP spirals/ties will prevent deterioration of the cover since these bars are more durable and do not corrode. Although this new technology is gaining popularity with designers, there is still a lack of experimental data, design procedures, and guidelines.

2 Experimental Program

Seventeen circular concrete columns, 356 mm in diameter and 1470 mm long were constructed and tested at the Structures Laboratories at the University of Toronto. All columns were reinforced laterally with GFRP spirals. Group 1 contained nine columns that were reinforced longitudinally with six 25 mm GFRP bars (Tavassoli et al. 2015), while group 2 contained eight columns that were reinforced with 6-25M steel bars. All seventeen columns were cast integrally with a 484 × 700 × 800 mm stub which represented a discontinuity like a beam column joint or a footing adjacent to the section of maximum moment. Refer to Figure 1 for a schematic of the specimen and column cross section.

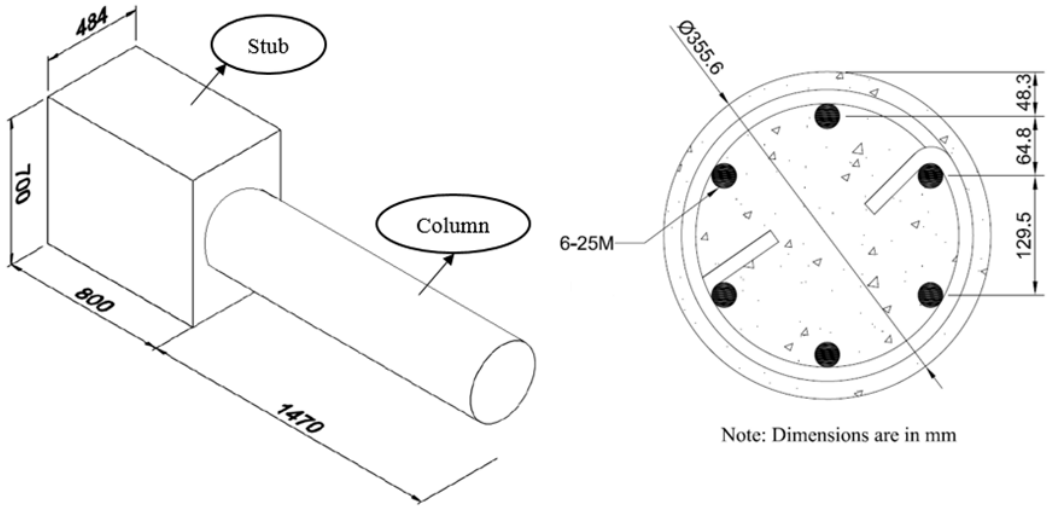

Figure 1: Specimen and cross-section of column

Due to the limitations of space, results from three columns from each group are discussed in this paper to highlight the effects of different variables including the type of longitudinal reinforcement, GFRP or steel. Table 1 provides general information regarding these six specimens.

Table 1: Specimen Details

Specimen (Group number)	Compressive Strength f'c (MPa)	Axial Load Level	Longitudinal Reinforcement	Lateral Reinforcement Size (mm) @ spacing (mm)	Lateral Reinforcement Ratio (%)
P28-C-12-50 (1)	35	0.28	GFRP	12 @ 50	3.00
P28-LS-12-50 (2)	40	0.28	Steel	12 @ 50	3.00
P28-C-12-160 (1)	35	0.28	GFRP	12 @ 160	0.95
P28- LS-12-160 (2)	40	0.28	Steel	12 @ 160	0.94
P42-C-12-160 (1)	35	0.42	GFRP	12 @ 160	0.95
P40-LS-12-160 (2)	40	0.41	Steel	12 @ 160	0.94

Table 2 and Table 3 provide information regarding the reinforcement material properties used in the aforementioned six specimens.

Table 2: Mechanical properties of longitudinal steel bars

Rebar type	Area A_S (mm^2)	Yield strength f_y (MPa)	Yield strain ε_y	Elastic modulus E_s (MPa)	Start of Strain hardening ε_{sh}	Ultimate strength f_u (MPa)	Strain at ultimate strength ε_u
25M	500	463	0.0025	194000	0.0086	645	0.14

Table 3: Mechanical properties of GFRP bars

Rebar type	Bar application	Nominal diameter mm (in)	Actual diameter mm (in)	Modulus of elasticity (MPa)	Ultimate stress (MPa)	Ultimate strain
GFRP	Spiral, Group 1	12 (0.472)	12.62 (0.497)	58399	1454	0.0249
	Spiral, Group 2	12 (0.472)	12.25 (0.482)	58500	1050	0.0179
	Longitudinal GFRP	25 (0.984)	25.11 (0.989)	65779	1087	0.0165

Figure 2 shows the group 2 specimens before test. The top part of the column is wrapped with carbon fiber reinforced polymer sheets in order to provide additional confinement to that area and to confirm that failure occurs within the instrumented test region close to the intersection of column and stub.

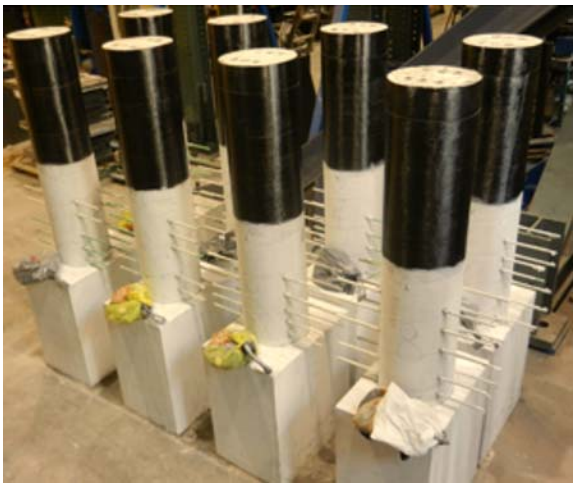

Figure 2: Specimens before test

Column Testing Frame (CTF), shown in Figure 3, was used for testing of specimens. The specimen were tested horizontally and subjected simultaneously to a constant axial load and cyclic quasi-static lateral displacement excursions. Figure 4 displays the lateral displacement protocol for testing of columns. The peak displacement of the first cycle was 0.75Δy, followed by two cycles each one to Δy, 2Δy, 3Δy, and so on. The nominal yield deflection, Δy, was calculated to be approximately 4 mm. An axial load of 1243 kN ($0.28P_0$) or 1775 kN ($0.41P_0$) was applied to group 2 columns in this project. P_0 is the nominal axial load capacity of column. Axial load was kept constant at the required level during the entire test. Lateral load was applied at the stub (approximately 150 mm away from the stub-column interface), so that the most critically loaded region of the column was adjacent to the stub and subjected to combined flexure, shear, and axial loading. Figure 5 presents a schematic drawing of a specimen in the horizontal test set up and it's relation to a portion of a column standing vertically in a real life application. The actual shear span of column is 1840 mm which extends from the stub-column interface to center of the right steel hinge. The shear span to depth ratio of the column was thus 5.17, where depth was defined as the outside column diameter.

Figure 2: Column Testing Frame (CTF)

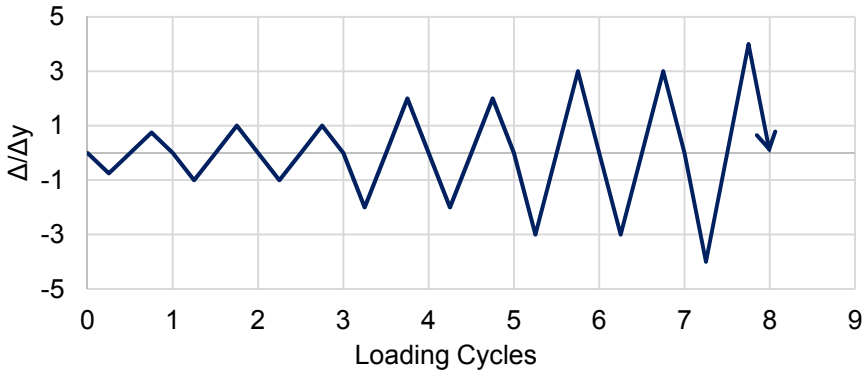

Figure 3: Lateral load excursions

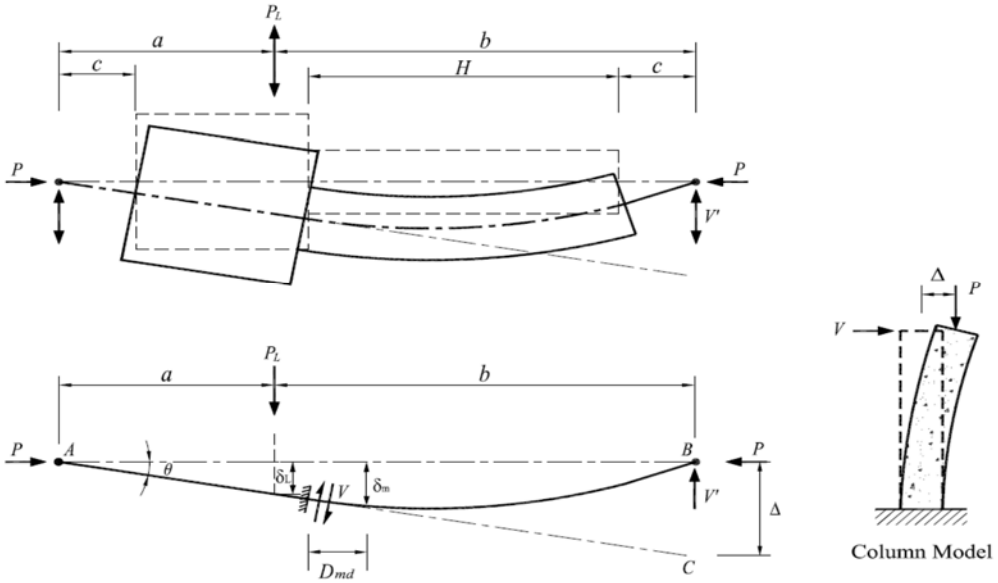

Figure 4: Schematic drawing of specimen under test

EMM-90-04

3 Experimental Results

The first visible sign of distress in group 2 specimens was the propagation of small cracks up to 0.3 mm in width. These flexural cracks were initiated on the tension face of columns as the tip deflection increased from 12 to 20 mm. The aforementioned cracks got wider during the next two cycles, and more small cracks were initiated. The width of cracks increased to 1 mm and approximately three flexural cracks at an average spacing of 120 mm were visible on the top and bottom faces by end of the 6th cycle.

The initiation of concrete cover spalling could be observed in the 6th lateral load cycle. Major spalling happened during the 7th cycle and large concrete pieces were detached from the core during the 8th cycle with max tip deflection of 45 mm. Spalling of concrete cover was more rapid for columns under higher axial load.

In group 1 specimens, the next main event was failure of the specimen. Lateral load was increased until the column was not able to hold the applied axial load. A combination of crushing and buckling of longitudinal GFRP bars in compression accompanied by crushing of concrete core in the most damaged zone led to a drop in axial load and termination of the test. No rupture was observed in the spirals.

In group 2 specimens, longitudinal steel bars buckled prior to rupture of GFRP spirals in columns with spiral pitch of 160 mm. In the specimen with spiral pitch of 50 mm, longitudinal bars buckled after spirals ruptured. The concept of premature buckling in longitudinal steel bars has been observed previously in square and rectangular columns (Bayrak and Sheikh 2001). They demonstrated that premature buckling could be prevented under cyclic loading only if the S/d_b ratio was no more than 6. This ratio indicates that premature buckling of a 25M bar occurs if the spiral pitch is greater than 150 mm which matches with experimental results from these tests.

The confinement provided to the core concrete and the support provided to the longitudinal bars vanishes as soon as the GFRP spiral is ruptured. A combination of buckling of the longitudinal bars in compression accompanied by the crushing of the concrete core in the most damaged zone led to termination of the test. Figure 5 shows the most damaged regions for the six specimens discussed here.

Figure 5: Columns after testing (in clockwise direction, starting from top left): P28-C-12-50, P28-C-12-160, P42-C-12-160, P28-LS-12-160, P41-LS-12-160, and P28-LS-12-50

Shear (V) vs. tip deflection (Δ) and moment (M) vs. curvature (Φ) hysteresis relations for all six columns are shown in Figure 7. The moment-curvature responses shown are for the most damaged sections of the columns. Although the maximum moment occurs at the column-stub interface, the damaged region is shifted slightly away from this interface due to the heavy confinement effect from the stub.

It is important to note that curvature in group 1 specimens is developed using the readings provided by the strain gauges installed on longitudinal bars, especially at large deformations, due to the fact that LVDTs became loose during the loading while in group 2 specimens, LVDTs measurements were used. The strain gauge readings in Group 1 specimens may have missed areas of greater deformations resulting in relatively lower curvature values.

- In group 1 and group 2 specimens:
  - Red horizontal line on the moment curvature response indicates the nominal unconfined moment capacity (M_n) of the section; compressive stresses in the longitudinal GFRP bars are also accounted for in the calculation of M_n in group 1 specimens
  - Slopped red line on the V-Δ represents the nominal shear capacity V_n with a decreasing slope caused by secondary P - Δ effects.
- In group 2 specimens:
  - Red dots indicate the initiation of small cracks up to 0.3 mm in width.
  - Light blue and dark blue dots represent the start of concrete cover spalling at bottom and top surfaces, respectively.
  - Green dots signify the rupture of spiral
  - Orange dots indicate that the longitudinal bar(s) had buckled
  - Purple dot indicates the shearing of longitudinal steel bar

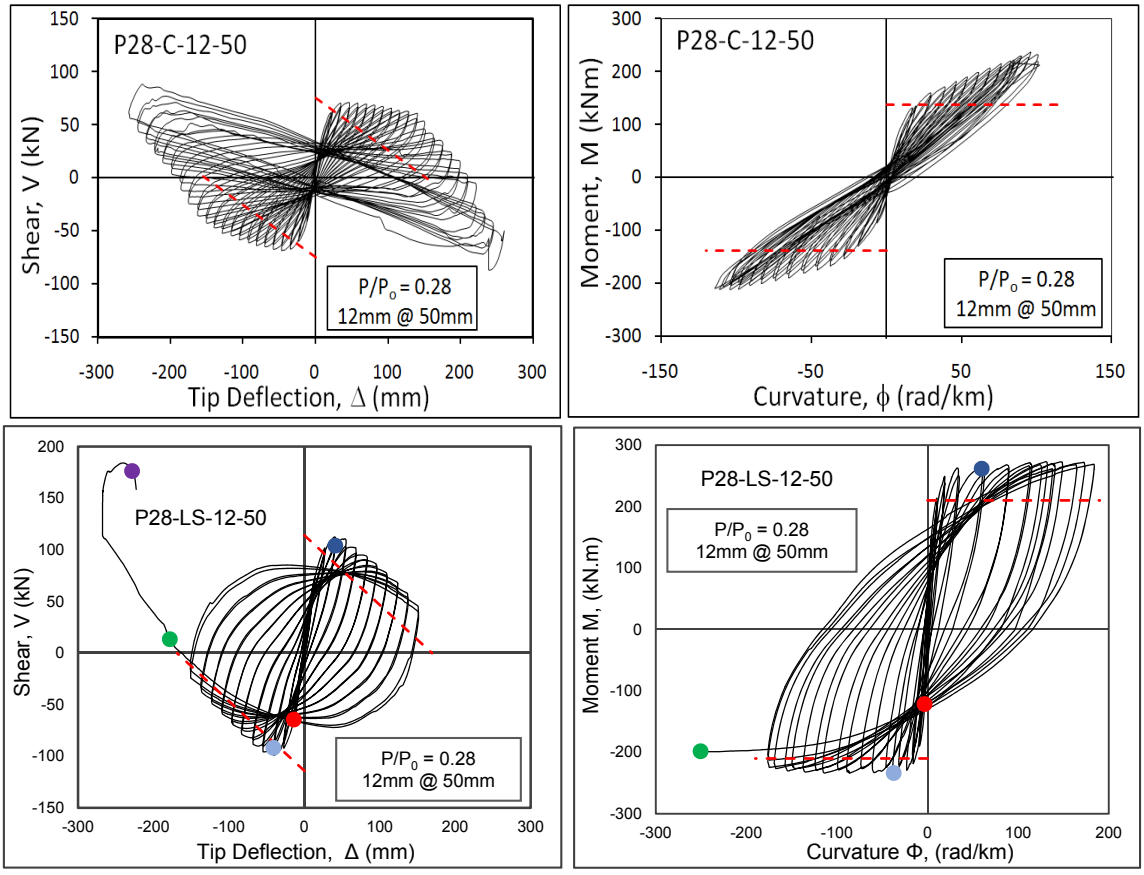

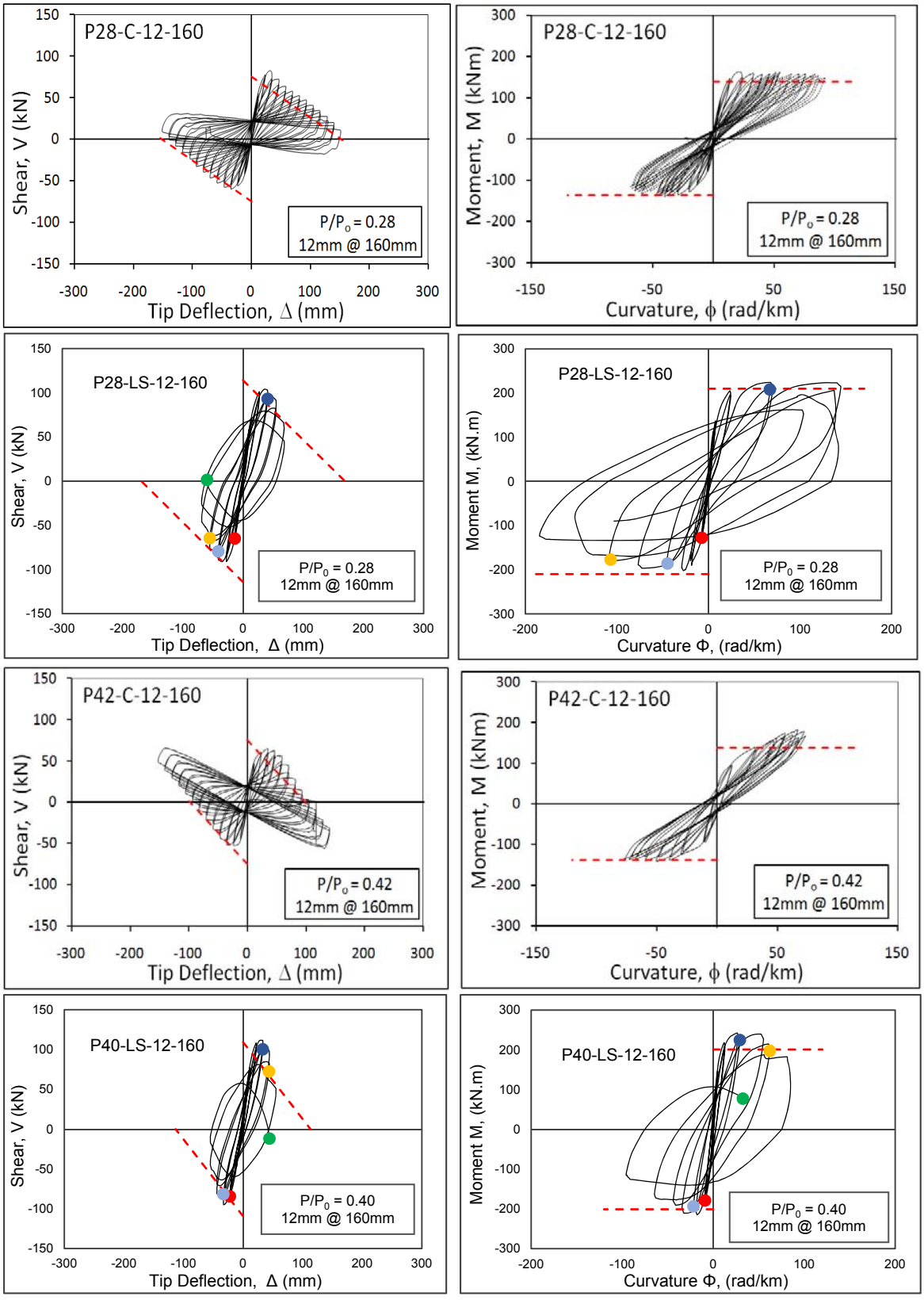

Figure 6: Shear vs. deflection and moment vs. curvature relations

Table 4 shows displacement ductility factor (μ_Δ), curvature ductility factor (μ_Φ), drift ratio (δ), maximum shear (V_{max}), maximum moment (M_{max}), and nominal moment capacity (M_n) for each specimen.

Table 1: Test Results

Specimen (Group number)	μ_Φ	μ_Δ	δ (%)	V_{max} (kN)	M_{max} (kN.m)	M_n	M_{MAX} / M_N
P28-C-12-50 (1)	> 10.0	6.7	7.3	70	224	125	1.79
P28- LS-12-50 (2)	33.8	4.7	4.7	106	254	210	1.21
P28-C-12-160 (1)	> 9.0	3.2	3.0	71	152	125	1.22
P28- LS-12-160 (2)	11.0	3.1	3.1	98	210	210	1.00
P42-C-12-160 (1)	> 5.3	3.7	3.0	59	162	125	1.31
P40- LS-12-160 (2)	9.5	3.1	2.6	103	225	201	1.12

4 Discussion

This study investigated application of corrosion-resistant GFRP spirals in circular concrete columns under constant axial load and cyclic lateral displacement excursions simulating earthquake forces.

Results from columns reinforced longitudinally with GFRP bars and laterally with GFRP spirals show that these columns can undergo several load cycles before failure and achieve high levels of deformability. For instance column P28-C-12-50 was designed for a drift ratio of 4% and achieved drift ratio of 7.3%. Due to the linear elastic behaviour of GFRP up to an approximate strain of 0.02, the concrete core and longitudinal bars were confined more effectively than they would be by steel spirals. This is mainly due to the fact that steel stiffness drops significantly after yield at a strain of 0.002. However, due to lower stiffness of the longitudinal GFRP bars, response of these columns was quite soft; therefore shear and moment capacities were lower compared to that of the conventional steel reinforced columns. The results improved significantly when longitudinal GFRP bars in group 1 specimens were replaced with steel bars in group 2 specimens.

Research has shown that the use of FRP transverse reinforcement improves corrosion resistance of a column due to non-corrosive properties of spiral GFRP and by adding an extra 15 mm of cover to longitudinal steel. These columns displayed flexural capacities that were approximately 30% higher than those of the comparable columns in group 1. Furthermore, the maximum shear reached is approximately 50% more when longitudinal GFRP bars in group 1 specimens were replaced with steel bars in group 2 specimens.

The magnitudes of the ductility parameters presented in Table 4 show that GFRP reinforced columns can be very ductile. Moreover, as the spiral spacing is decreased from 160 mm to 50 mm, all ductility parameters increased considerably. It is also important to note that columns are less ductile under higher axial loads.

5 Conclusion

Application of GFRP spirals mitigates the corrosion of steel reinforcement in concrete and hence improves the durability of the structure. Results from this research show that GFRP spirals can be used as primary lateral reinforcement for shear and confinement in concrete columns designed for seismic resistance even when they are subjected to large axial loads. Use of GFRP bars as longitudinal reinforcement results in significantly softer response of columns and lower strength compared with that of columns reinforced with steel bars.

6 Acknowledgements

The financial support for this work was provided by IC-IMPACTS, an NSERC network of Centres of Excellence. The NSERC scholarship and Alexander Graham Bell Canada Graduate Scholarship awarded to the first author are also gratefully acknowledged. The experimental work reported here was carried out in the Structures Laboratories of the University of Toronto.

7 References

Bayrak, O., and Sheikh, S.A., 2001, “Plastic Hinge Analysis”, Journal of Structural Engineering, ASCE, 127(9), pp. 1092-1100.

Hays, G. F., (2010) NACE-International, The corrosion society. http://events.nace.org/euro/corrodia/Fall_2010/wco.asp (Jan. 09, 2015)

Tavassoli, A., Liu, J., Sheikh, S.A., (2014) “Glass Fiber-Reinforced Polymer-Reinforced Circular Columns under Simulated Seismic Loads.” ACI Structural Journal, V. 112, No. 1, Jan-Feb, 2015, 103-114.